HHS Public Access

Author manuscript

Nat Immunol. Author manuscript; available in PMC 2012 September 01.

Published in final edited form as:

Nat Immunol. ; 13(3): 264–271. doi:10.1038/ni.2230.

Elevated and sustained Egr1 and Egr2 expression controls NKT lineage differentiation in response to TCR signaling

Michael P. Seiler[1], **Rebecca Mathew**[1], **Megan K. Liszewski**[1], **Chauncey Spooner**[1,2], **Kenneth Barr**[1], **Fanyong Meng**[1], **Harinder Singh**[1,2], and **Albert Bendelac**[1]

[1]Committee on Immunology and The Howard Hughes Medical Institute, University of Chicago, Chicago IL, 60637, USA

Abstract

TCR-driven interactions determine the lineage choice of $CD4^+CD8^+$ thymocytes, but the molecular mechanisms that induce the lineage-determining transcription factors are unknown. Here we show that TCR-induced Egr2 and Egr1 proteins had elevated and prolonged expression in NKT lineage precursors compared with conventional lineages. ChIP-seq analysis uncovered that Egr2 directly bound and activated the promoter of *Zbtb16* which encodes the NKT lineage-specific transcription factor PLZF. Egr2 also bound the *Il2rb* promoter and controlled the responsiveness to IL-15, which signals the terminal differentiation of the NKT lineage. Thus, we propose that elevated and persistent Egr2 levels specify the early and late stages of NKT lineage differentiation, providing a discriminating mechanism that enables TCR signaling to instruct a thymic lineage.

NKT cells are a conserved population of innate-like T cells that recognize CD1d-lipid complexes and rapidly produce an extensive assortment of cytokines and chemokines capable of modulating immunity to multiple conditions including infection, cancer, autoimmunity and allergy [1, 2]. Most NKT cells express a canonical TCRα chain, $V_\alpha14\text{-}J_\alpha18$, which arises randomly during thymic development at the $CD4^+CD8^+$ double positive (DP) stage and, together with TCR Vβ8, Vβ7 or Vβ2 chains, confers specificity for self lipid ligands expressed by cortical thymocytes to instruct NKT lineage differentiation. Tetramers of CD1d complexed with the synthetic ligand α-galactosylceramide (αGalCer), a mimetic of microbial lipid antigens, readily identify the rare NKT precursors that have just undergone

---

Corresponding Author: Albert Bendelac, abendela@bsd.uchicago.edu.
[2]Current Address: Department of Discovery Immunology, Genentech

ACCESSION CODES

ChIP sequencing data available at Gene Expression Omnibus, GSE34254.

CONTRIBUTIONS

M.P.S. designed and performed experiments and analyzed the data; R.M. did the ChIP-seq experiment in Fig. 3; M.K.L. assisted in doing experiments in Fig. 1. C.S. and H.S. assisted with the design and interpretation of experiments, provided constructs, reagents and mouse strains. K.B. analyzed the ChIP-seq experiment in Fig. 3; F.M. assisted in doing experiments; A.B. designed and supervised experiments and data analysis. M.P.S. and A.B. wrote the manuscript

COMPETING FINANCIAL INTERESTS

The authors declare no competing financial interests.

positive selection in the thymus [3]. This so-called “stage zero” is characterized by a $CD4^+CD69^+CD24^{hi}$ phenotype equivalent to that of the transitional stage of MHC-restricted T cells (CD4t). Stage 1 cells down-regulate CD24 and have a $CD44^{lo}$ naïve phenotype equivalent to mature CD4 single positive thymocytes. However, these cells have already initiated a program of cell division and effector differentiation, which culminates at stage 2 when cells have a memory-like $CD44^{hi}$ phenotype and leave the thymus. Progression to stage 3 is marked by the cessation of cell division and the acquisition of an NK-like program. This terminal differentiation occurs in the periphery, although a small fraction of cells can remain resident in the thymus where they also differentiate to stage 3.

As in other αβ lineage T cells, TCR signaling is thought to instruct NKT lineage development through the expression of signature transcription factors. The transcription factor PLZF, which is encoded by *Zbtb16*, directs the acquisition of the NKT cell effector program during development, including their cytokine and migratory properties [4–7]. The expression of PLZF in thymic NKT development is tightly regulated, as it is first induced in 40% of stage zero cells and is expressed at peak levels in 100% of stage 1 and stage 2 cells. Mutations of *Zbtb16* abrogate the memory-effector differentiation of NKT cells, resulting in their reversal to a naïve phenotype and redistribution to the lymph nodes rather than the liver and other organs where they normally predominate. Moreover, constitutive expression of equivalent levels of PLZF during thymic development induces the effector program in all conventional T cells independently of their antigen specificity [8]. Thus, PLZF represents a pivotal signature transcription factor of the NKT cell lineage. Given the temporal proximity of PLZF expression to lineage bifurcation, we hypothesized that the transcriptional control elements required for PLZF expression would be among the earliest determinants of lineage commitment.

While differences in TCR signaling are thought to instruct the expression of lineage-determining factors such as *Zbtb7b* encoding c-Krox/Th-POK for the $CD4^+$ T cell lineage, or *Foxp3* for regulatory T cells, the identities of the signaling molecules involved in gene regulation are unknown. The Egr family members Egr1, Egr2 and Egr3 are among the earliest transcription factors induced by TCR signaling and their redundant role in activating the survival program associated with the positive selection of T cells is well established [9–11]. Thus, the combined ablation of Egr1 and Egr2 impairs the thymic generation of T cells as well as NKT cells. Ablation of Egr2 alone, however, was sufficient to significantly impair survival of NKT cells but not of conventional T cell precursors, implying some unique function of this factor in the NKT lineage [12, 13]. Further, the absence of lineage rescue by transgenic expression of Bcl-2 [13] suggested a direct role for Egr2 in lineage differentiation, as previously shown, for example, in myeloid precursors where Egr2 is at the center of a transcriptional regulatory network promoting macrophage genes and repressing neutrophil genes [14].

In this study, we demonstrate elevated and sustained expression of Egr2 and, to a lesser extent, Egr1 proteins in NKT precursors compared with conventional T cells undergoing positive selection. ChIP-seq analysis revealed that Egr2 directly bound and activated the promoter of *Zbtb16*, resulting in PLZF protein expression. Furthermore, we uncovered a crucial role of Egr2 in conferring responsiveness to interleukin 15 (IL-15). These findings

identify a direct link between TCR signaling and the key stages of commitment and differentiation in the NKT lineage.

RESULTS

Elevated Egr expression in NKT cell thymic precursors

Measuring the natural levels of TCR signaling intermediates in thymocytes represents a technical challenge because of the weak and transient nature of signaling during development and the limiting numbers of cells at different stages. We used confocal imaging of single cells to quantify and compare the expression of Egr2 protein during the development of conventional T cells and NKT cells. At the $CD24^{hi}CD69^{hi}CD4^{+}$ stage immediately following TCR engagement by natural ligands *in vivo* (so-called transitional CD4 (CD4t) for MHC-restricted T cells or also stage 0 for NKT cells), both lineages induced Egr2 above the baseline levels of DP thymocytes, but $V_{\alpha}14$ transgenic cells expressed Egr2 at twice the level of wild-type T cells on average (Fig. 1a). Even after developing past the $CD24^{lo}CD44^{lo}NK1.1^{-}$ stage 1 and maturing to the $CD24^{lo}CD44^{hi}NK1.1^{-}$ stage 2 immediately preceding thymic emigration, $V_{\alpha}14$ transgenic cells maintained higher Egr2 levels than the equivalent $CD24^{lo}$ stage of MHC-restricted CD4 single positive thymocytes (Fig. 1b). In fact, at all stages of development and maturation, including the $CD24^{lo}CD44^{hi}NK1.1^{+}$ stage 3, which represents the terminal NK-like differentiated state of this lineage, NKT thymocytes identified by tetramer staining (Tet^{+}) expressed more Egr2 than conventional T cells (Fig. 1c). These confocal microscopy findings were confirmed by intra-cellular flow cytometry analysis using a different monoclonal anti-Egr2 antibody (Fig. 1d). A similar increase was detected for Egr1, although the elevation significantly subsided at stage 1 (Fig. 1e). Thus, NKT thymocytes exhibited a greater and more sustained post-selection rise in Egr levels than MHC-restricted thymocytes.

Strong TCR signals induce Egr2 and PLZF *in vivo*

Because Egr1 expression is dependent on the Ras-MAPK pathway and Egr2 is mainly dependent on the NFAT pathway downstream of TCR signaling [9, 12, 15], the data suggested that NKT cell development is promoted by elevated TCR signaling, both in quantity and in duration. This conclusion is consistent with previous reports showing that the NKT cell TCRs are autoreactive and recognize agonist self lipid ligands [16, 17]. We explored whether, in addition to the reported survival effects, Egr2 might function to regulate NKT cell fate determination by regulating the induction of PLZF, the signature transcription factor of NKT cells. To test the potential link between TCR signaling, Egr2 induction and subsequent PLZF expression, we injected anti-TCRβ antibody *in vivo* and examined the relative expression of Egr2 and PLZF in signaled ($CD69^{+}$) thymocytes. *Egr2* mRNA was rapidly induced after 30 minutes, reached a maximum at 1 hour post injection and remained measurably elevated 24 hours later (Fig. 2a). *Zbtb16* mRNA was upregulated with some delay, as it was detectable at 18 and 24 hours (Fig. 2b). Egr2 protein could also be detected in whole thymocytes by immunoblotting and in DP thymocytes by flow cytometry (Fig. 2c,d). We further tested whether *Zbtb16* induction depended on Egr proteins. Because a complete block of NKT cell development required the ablation of both Egr1 and Egr2 [13], we

used *Egr1*$^{-/-}$ *Egr2*$^{fl/fl}$Lck-cre double mutant mice (*Egr1-Egr2* DKO) as recipients of anti-TCRβ antibody. *Egr1-Egr2* DKO thymocytes exhibited an 80% decrease of *Zbtb16* induction on average compared with wild-type over multiple independent experiments (Fig. 2e). We noted residual *Egr2* expression after antibody injection into DKO mice, which we attribute to incomplete cre-mediated excision of *Egr2* in some cells (see below in Fig. 5a). Thus, although this experimental model does not rule out possible cell-extrinsic effects, the data suggest that TCR agonist signaling was associated with rapid induction of *Zbtb16* mRNA in an Egr-dependent manner in thymocytes *in vivo*.

Egr2 binds to critical NKT lineage genes *in vivo*

To test the possibility that *Zbtb16* might be a direct target of Egr2, we performed unbiased, genome-wide studies of Egr2 binding by ChIP-Seq on NKT thymocytes isolated from pools of $V_{\alpha}14$ transgenic mice [18] or on total thymocytes of anti-TCRβ injected mice (data available online at Gene Expression Omnibus, GSE34254). The NKT dataset yielded fewer binding events (i.e. peaks) than the TCRβ-injected thymocytes (Fig. 3a), an anticipated outcome due to the lower level of endogenous Egr2 and the limiting numbers of NKT thymocytes that could be recovered. Nevertheless, when both datasets were surveyed for the most frequently enriched motifs, the sequences identified were essentially the same and were identical to the canonical Egr2 binding motif [19]. Further, the two datasets showed similar patterns of binding with substantial overlap of bound genes, particularly at promoters (Fig. 3b–d).

To identify Egr2 target genes with high probability of involvement in NKT cell development, we compared the list of gene-associated peaks (excluding intergenic peaks) in both ChIP-Seq data sets with the list of genes showing >1.8 fold expression at NKT stages 1, 2 and 3 over CD4 SP thymocytes. Finally, we further limited the study to genes with a conserved Egr2 binding motif in human. This analysis led to a shortlist of nine Egr2 target genes that were specifically upregulated during NKT development (Table I). Four of these genes are known to be pivotal for NKT cell development or function and were bound by Egr2 in their promoter region (Fig. 3e). They included *Zbtb16* encoding PLZF; *Il2rb* encoding the beta chain of the IL-15 receptor, which is essential for the expression of NK receptors and the survival of terminally differentiated stage 3 NKT cells [20–22]; *Fasl* encoding Fas ligand, a known target of Egr2 [15]; and *Ccnd2* encoding the cell cycle regulator cyclin D2 which is essential for the expansion of NKT thymocytes. Thus, unbiased genome-wide studies revealed direct binding of Egr2 to the promoters of critical NKT lineage genes during development.

Egr2 directly trans-activates *Zbtb16* expression

A conserved consensus Egr binding motif was located upon sequence examination of the *Zbtb16* proximal promoter at ~240 base pairs upstream of the TSS (Fig. 4a). Binding in this region was further confirmed by ChIP-qPCR (Fig. 4b). Moreover, an oligonucleotide encompassing the putative binding site (highlighted in Fig. 4a) was directly shown to bind *in vitro* translated Egr2 by electrophoretic mobility shift assay in a sequence-specific manner (Fig. 4c). Furthermore, upon co-transfection of *Egr2* with a *Zbtb16* promoter-driven luciferase plasmid in KG1a cells, luciferase expression was strongly induced and depended

on the presence of the Egr2 binding site, providing functional evidence that Egr2 can activate the *Zbtb16* promoter (Fig. 4d). Taken together, these results establish that Egr2 is a direct transactivator of the *Zbtb16* promoter.

Egr2 regulates distinct NKT developmental transitions *in vivo*

Based on this unbiased analysis of Egr2 binding, we next examined the effect of Egr2 ablation on NKT lineage checkpoints in the mouse thymus. To minimize the well-known redundancy and compensation between Egr proteins, we studied the effects of single and double *Egr1* and *Egr2* ablation in competitive radiation chimeras reconstituted with a 1:1 mixture of mutant ($CD45.2^+$) and wild-type ($CD45.1^+$) bone marrows. In this experimental system, Egr1-deficient NKT cells developed normally, whereas Egr2-deficient thymocytes were arrested between developmental stage 2 and 3 (Fig. 5a). In contrast, *Egr1-Egr2* DKO thymocytes were sharply arrested earlier, at stage 1 (Fig. 5a). These precise developmental blocks were reproduced in multiple experiments (Fig. 5b) and are generally consistent with previous reports [12, 13], although we found that the competitive bone marrow chimeras revealed sharper and more consistent developmental blocks than the germline mutant mice, which sometimes showed leaky phenotypes and incomplete blocks.

Egr2 controls PLZF expression

The early block in *Egr1-Egr2* DKO thymocytes was reminiscent of the defect observed in mice lacking the NKT lineage-specific transcription factor PLZF [4, 5]. Indeed, whereas PLZF expression is tightly controlled during NKT development, beginning as early as stage 0 and present at high levels in 100% of stage 1 cells, it was conspicuously absent in the stage 1-arrested *Egr1-Egr2* DKO NKT cells (Fig. 6a). Very few cells progressed to stage 2, and the majority of those that did were ROSA26 negative, suggesting failure to delete the *Egr2* allele (Fig. 5a, bottom row). In contrast, PLZF was normally induced in both Egr1 and Egr2 single deficient NKT thymocytes, indicating that Egr1 can compensate for the loss of Egr2 during early NKT development (Fig. 6a). These observations were consistent across multiple independent sets of chimeras examined (Fig. 6b). Together with the ChIP-Seq data and the promoter transactivation studies, these results indicated a direct and critical function of Egrs in PLZF induction.

Egr2 controls IL-2Rβ expression

The late developmental block observed in Egr2-deficient thymocytes was reminiscent of the defects associated with abrogation of IL-15 signaling, as reported in studies of IL-15, IL-15Rα and T-bet mutant mice [20–22]. IL-15 controls the stage 2 to 3 transition that is defined by the acquisition of the NK-like properties intrinsic to the NKT lineage. Using biotinylated double-stranded oligonucleotides and *in vitro* translated Egr2 protein in a streptavidin bead pull-down assay, we directly showed that Egr2 could bind the promoter of *Il2rb* in a sequence-specific manner (Fig. 7a). The same assay confirmed the binding of Egr2 to the PLZF promoter and the Egr2 consensus oligonucleotide probe, as previously shown by electrophoretic mobility shift assay (Fig. 4c). *In vivo*, Egr2-deficient NKT cells failed to up-regulate IL-2Rβ (CD122) compared with their wild-type counterparts in 1:1 mixed chimeras (Fig. 7b). To facilitate the analysis of developmentally arrested Egr2-

deficient NKT thymocytes, we crossed the *Egr2*$^{fl/fl}$*Lck-Cre* (*Egr2*$^{\Delta/\Delta}$) onto the $V_{\alpha}14$ transgenic background and generated chimeric mice using an equal mixture of total bone marrow from Egr2-deficient $V_{\alpha}14$ transgenic (CD45.2^{+}) and Egr2-sufficient $V_{\alpha}14$ transgenic (CD45.1^{+}) as donors. Consistent with a defect in IL-2Rβ upregulation, Egr2-deficient NKT cells failed to upregulate the NK family receptors NK1.1 and NKG2D to levels observed in wild-type (Fig. 7c). qRT-PCR analysis in Egr2-deficient and Egr2-sufficient stage 2 NKT cells purified from these mixed chimeras revealed a down regulation of *Id2* in the absence of Egr2 (Fig. 7d–e). This result is consistent with a function for Id2 in NKT survival and in acquisition of the NK program[23–25]. This analysis also revealed a 2-fold increase of *Egr1* mRNA in the Egr2-deficient cells (Fig. 7e). Egr1 protein upregulation in Egr2-deficient cells was confirmed by confocal microscopic analysis of single cells (Fig. 7f), suggesting that compensatory mechanisms promoted Egr1 expression at the transcriptional level in the absence of Egr2. Thus, Egr2 directly controlled the induction of IL-2Rβ at the late stage of NKT cell development.

DISCUSSION

Previous reports indicated that Egr2 was selectively required for the survival of developing NKT thymocytes. Here we show that elevated and sustained Egr2 expression is induced downstream of TCR signaling in NKT precursors and Egr2 is directly connected with the key molecular checkpoints defining NKT lineage commitment and stage progression. These results suggest that Egr2 not only induces the early lineage-defining transcription factor PLZF, but also controls the downstream expression of the IL-2Rβ chain.

PLZF directs the acquisition of effector properties, such as upregulation of CD44, downregulation of CD62L and dual production of IL-4 and IFN-γ, that define the progression from stage 1 to stage 2, but other factors, including Egr1 and Egr2, are required to promote survival and induce the rounds of cell division that characterize this transition. Likewise, IL-2Rβ is required for responsiveness to IL-15 and the subsequent terminal differentiation to stage 3, but its expression is only part of the program controlling the terminal differentiation of NKT thymocytes. More intricate connections defining the regulatory network presiding over NKT cell fate commitment and differentiation are expected. For example, Egr2 was essential for the upregulation of *Id2*, which is not only important for NKT cell survival in the periphery [24] but is also critical for NK cell differentiation [23, 25]. Studies in myeloid cells have shown binding of PLZF to the *Id2* promoter [26] and, in preliminary studies of human NKT cells, ChIP-seq analysis identified binding of Egr2 to a conserved Egr binding site in the promoter of *Id2* (data not shown), highlighting potential common targets of Egr2 and PLZF in the cooperative orchestration of NKT cell development.

Although Egr2 is clearly central to NKT cell development, our studies did not fully elucidate the precise role of Egr1 in wild-type NKT thymocytes. Egr1 expression is also elevated at the earliest stages of NKT development and might contribute to PLZF induction in a redundant manner with Egr2. Alternatively, Egr1 might only be recruited to the PLZF promoter in Egr2-deficient thymocytes because of its compensatory increase in the absence of Egr2. There is precedent for such compensatory pathways between Egr proteins in T

cells [27] and additional studies have suggested a cross-talk between the calcineurin pathway upstream of Egr2 and MAP kinase signaling upstream of Egr1 during thymocyte development [28]. Finally, Egr1 might activate other mechanisms that redundantly control PLZF induction. The redundancy between Egr1 and Egr2 was observed for the induction of PLZF, but not for IL-2Rβ where Egr2 alone was required, thus allowing the identification of two Egr-controlled checkpoints in NKT cell development.

The tight developmental sequence linking positive selection of NKT thymocytes with elevated Egr2 and Egr1 induction and PLZF upregulation strongly suggests that TCR signaling by agonist self ligands is the trigger of this differentiation pathway. This hypothesis is supported by the experimental induction of PLZF mRNA in an Egr-dependent manner after *in vivo* injection of agonist anti-TCRβ antibody. It is also consistent with a previous report of PLZF protein induction in γδ T cells by anti-TCR antibody in an *in vitro* OP9 stromal cell-based culture assay [29]. The extent to which other TCR signaling branches are overstimulated during NKT cell development is unclear at present and awaits single cell studies of other signaling molecules. It is noteworthy in that respect that nur77, another early gene induced by TCR activation was found to be increased in NKT thymocytes based on a GFP-reporter system [30].

TCR signaling in developing NKT cells occurs in the context of homotypic interactions between thymocytes, with recruitment of Slam family member signaling through the adaptor SAP and the kinase Fyn [18, 31]. SAP-deficient mice exhibit a massive NKT cell developmental arrest at stage 0, but some induction of *Zbtb16* was nevertheless observed [4], suggesting that Slam-SAP signaling may not be required. However, a role of this signaling pathway in sustaining a high level of Egr2 expression should be explored.

In addition to the early elevation of Egr2, which was important for PLZF induction, Egr2 expression was critical for the activation of IL-2Rβ and transition to stage 3 at a later time point in development. Whether continued TCR signaling or additional regulatory pathways were responsible for sustained Egr2 expression is unclear. For example, MiR-150, which is selectively downregulated in NKT cells [32], was reported to suppress Egr2 in gastric cancer cells [33]. In addition, other mechanisms regulating Egr2 and involving nab2 and Gfi-1 have been reported in myeloid cells [14].

Various studies have suggested that differences in TCR signaling, perhaps due to recognition of agonist ligands, underlie the unique developmental programs of T cell subsets such as NKT cells, gamma-delta T cells, intestinal intraepithelial CD8αα TCRαβ cells and T_{reg} cells [34–37]. Few studies, however, have identified critical links between TCR signaling elements and lineage commitment. For example, whereas NFAT and c-Rel are important for Foxp3 induction in the T_{reg} lineage [38–40], increased activation of these pathways has not been demonstrated. Moreover, a specific role for Egr3 has been proposed in the development of epidermal γδ T cells, but its expression pattern and the gene regulatory network employed by Egr3 in this context remain unknown [41].

Our results not only provide molecular evidence for increased TCR signaling in NKT cell precursors, but also identify a direct connection between an early signaling-dependent

transcription factor and the induction of signature genes that control key checkpoints in NKT cell development. Similar mechanisms whereby the intensity and duration of signaling is translated into distinct lymphoid cell fates [42, 43] are likely to operate in other models of lymphoid differentiation.

METHODS

Mice

Egr1$^{-/-}$*Egr2*$^{fl/fl}$*lck-cre*$^{+}$,*ROSA26*$^{+}$ mice obtained from Dr. Patrick Charnay (INSERM, France) have been described [46]. C57BL/6 (CD45.2) and B6.SJL-PtprcaPep3bBoyJ (CD45.1) were from the Jackson laboratory. The B6. V_{α}*14*-TG mice with a *cd4* promoter driving expression of the $V_{\alpha}14$-$J_{\alpha}18$ TCR α chain were generated and maintained in our laboratory [18]. All mice were raised in a specific pathogen-free environment at the University of Chicago and experiments were performed in accordance with the guidelines of the Institutional Animal Care and Use Committee.

Generation of Mixed Bone marrow Chimeras

Six- to eight-week old B6 (CD45.1), or B6.*CD1d*$^{-/-}$ mice were subjected to 1000 Rads irradiation with a gamma cell 40 irradiator with a cesium source. Three to six hours later, irradiated mice were injected i.v. with 2×10^{6} cells containing a 1:1 mixture of bone marrow cells from mutant (*Egr1*$^{-/-}$), (*Egr2*$^{fl/fl}$,*Lck-Cre*$^{+}$), (*Egr1*$^{-/-}$, *Egr2*$^{fl/fl}$,*Lck-Cre*$^{+}$,*ROSA*$^{+}$), (V_{α}*14*-TG,*Egr2*$^{fl/fl}$,*Lck-Cre*$^{+}$) and WT (CD45.1) or V_{α}*14*-TG (CD45.1) mice. Mice were analyzed after 6 weeks.

Flow cytometry

CD1d-αGalCer tetramers were obtained from the NIH tetramer facility or prepared as described [47]. Fluorochrome-labeled monoclonal antibodies against mouse B220 (RA3-6B2), CD3e(17A2), CD4(L3T4, or GK1.5), CD8a (53-6.7), CD11c (HL3), CD24 (M1/69), CD44 (IM7), CD45.1 (A20), CD45.2 (104), NK1.1 (PK136), TCRb (H57) NKG2D (CX5), CD122 (TM-β1), CD69 (H1.2F3) were purchased from eBioscience, BD Biosciences, or BioLegend.

For MACS enrichment, thymocytes were labelled with APC-conjugated CD1d-αGalCer tetramers, or anti-CD69, and enriched on an autoMACS cell separator (Miltenyi Biotech), as described [3], with all procedures conducted on ice. Samples were analyzed on an LSRII (Becton Dickinson) or sorted on a FACSAria II (Becton Dickenson). Intracellular staining of PLZF was performed as described [4]. For intracellular staining of Egr2, cells were prepared using the Foxp3 fixation/permeabilization kit (eBioscience) and stained with PE-conjugated mAb erongr2 (eBioscience).

Confocal Microscopy

Cells were isolated by magnetic enrichment and/or FACS with all procedures conducted on ice. Briefly, thymocytes from either C57B6/J or V_{α}*14*-TG mice were CD8 depleted using anti CD8 microbeads (Miltenyi) according to manufacturers protocol. Cells were stained for CD4, CD24, CD8, and CD69, and sorted as CD4^{+}CD8^{-}CD24^{hi}CD69^{+} (CD4 transitional), or

$CD4^+CD8^-CD24^{lo}CD69^-$ (CD4SP). CD8 single positive thymocytes were collected after sorting CD4 and CD8 stained thymocytes. $V_\alpha 14$-TG thymocytes were enriched with Tetramers and MACS, and stained for CD24, NK1.1, and CD44. Sorted cells were adhered to glass slides by cytospin, dried at room temperature before fixing for 15 minutes with 4% paraformaldehyde, followed by 3 washes with PBS. Cells were then incubated with 0.5% Triton in PBS for 10 minutes, washed and blocked with 10% normal donkey serum and 1% BSA for 1 hour. Cells were stained with 1 μg anti-Krox20 (Egr2) (Covance) antibody, 200 ng anti-Egr1 (SC-110X from Santa-Cruz) or IgG control for 2 hours at RT, washed with PBS and incubated with 1:250 dilution of donkey anti rabbit Alexa-555 secondary antibody (Invitrogen) for 30 minutes at RT, washed and mounted with prolong gold mounting solution (Invitrogen). Slides were dried over night at RT and imaged on an Olympus IX81 laser scanning confocal microscope with 60× oil objective. Image acquisition was at 2.5× or 10× (micrographs) digital zoom. Fluorescence intensity per cell was measured using ImageJ software (NIH) applied to randomly chosen DAPI positive nuclei.

SDS-PAGE and Western Blotting

Thymocytes (5×10^6) were centrifuged and frozen at −80 C until use. Cell pellets were lysed on ice in TNE lysis buffer containing protease inhibitors before separation by SDS-PAGE on a 10% pre-cast minigel (BioRad). The gel was transferred to PVDF membrane and blotted with 0.1 mg/ml anti-Krox20 (Egr2) (Covance) antibody. Goat anti-rabbit-HRP secondary was applied at 0.08 mg/ml (111-036-003;Jackson ImmunoResearch), and HRP was detected by chemiluminescence (alpha Innotech).

Gel shift mobility assays

In vitro translated Egr2 was generated with the TNT coupled reticulocyte lysate system (Promega). IVT extracts were incubated with 5′-biotinylated double stranded oligonucleotides purchased from IDT containing an optimal Egr2 binding site (Egr2 consensus; 5′ TCG ACT GTG TAC GCG TGG GCG GTT), or the 25 nucleotide sequence flanking the putative Egr2 binding site within the *Zbtb16* core promoter (*Zbtb16* (Egr2bs): 5′CAGGCACGCACACCCACCCCAAGCTCCAGGC), or a binding site mutated double-stranded oligonucleotide (*Zbtb16* (Egr2Δ bs): 5′CAGGCACGCACAGCCAGCCCAAGCTCCAGGC) and reactions performed according to manufacturers instructions using the LightShift Chemiluminescent EMSA kit (Pierce). After the reaction, samples were mixed with 5 μl sample loading buffer and run on pre-cast DNA retardation gels (6% Polyacrylamide, Invitrogen), and transferred for 1 hour to nitrocellulose in Novex® TBE Running Buffer (0.5X) (Invitrogen). After cross-linking, the biotinylated oligonucleotides were detected according to the EMSA kit (Pierce). Super-shift was detected by adding 1μg anti-Egr2 antibody (Covance) to the binding reaction [15].

dsDNA probe pull-down and western blot analysis

Ten microliters of in vitro translated Egr2 was incubated with 1 μg of biotinylated dsDNA probes for 1 hour at 4 °C on a rotator. *Zbtb16* (Egr2 bs), *Zbtb16* (Egr2Δ bs) and consensus oligonucleotides were the same as described for EMSA. *Il2rb* (Egr2 bs): 5′ATAAGATCTCCTCCTACGCCCAGGGGC A 3′; *Il2rb* (Egr2Δ bs):

5′ATAAGATATATATATACGCCCAGGGGC A-3′. Sepharose streptavidin beads were added to the extracts and incubated at 4 °C for 40 min. The beads were collected by centrifugation and washed three times with PBS, 0.05% NP40. 2×SDS-loading buffer was added and the extracts were subjected to SDS–PAGE and western blot with anti Egr2 antibody.

Transient transfection and reporter assays

The proximal promoter of mouse *Zbtb16* (−740 to +173) was cloned into the pGL3-basic and pGL3-enhancer (containing a 3′ SV40 viral enhancer) vectors (Promega). To disrupt the Egr2 binding site, a site directed mutagenesis kit (Stratagene) was used to change the sequence from 5′ CACCCACCG 3′ to 5′ CTATTTATC 3′ (mutated binding site, mut.bs) in the pGL3 enhancer construct. These plasmids were transfected along with a cmv-renilla luciferase plasmid into KG1a cells (ATCC) using the Amaxa 96-well nucleofector kit (Lonza). Reporter assays were performed using the dual luciferase detection system (Promega), and firefly luciferase levels were normalized to renilla luciferase values.

ChIP Sequencing

Chromatin from 2×10^7 cells was used for each ChIP experiment. Purified DNA from Egr2 ChIP and Input were prepared for sequencing following the Illumina Genomic DNA protocol. 8 pmoles of DNA library was applied to each lane of the flow cell and sequenced on Illumina GAII sequencer according to manufacturer's protocols.

Illumina image extraction pipeline software was used to identify cluster positions, perform base calling and generate QC statistics. Eland Extended was used to align sequences to mouse genome (NCBI 37/mm9). Non-unique sequences that aligned to more than two different locations were discarded prior to subsequent analysis. QuEST was used to identify enriched binding regions or peaks [48]. Hypergeometric Optimization of Motif EnRichment (HOMER) was used for motif identification by extracting "peak associated sequences" comprised of the 200 bp surrounding each peak call [49]. HOMER was applied with all default parameters to yield significantly overrepresented motifs. Alignment images were generated using the UCSC genome browser[50].

qRT-PCR

Total RNA was isolated from 20,000–100,000 purified thymic subsets with a combination of Trizol (Invitrogen), RNeasy kit (Qiagen) and reverse transcribed using the affinity Script qPCR cDNA synthesis kit (Stratagene). qPCR primer pairs for *Egr1*, *Egr2* and *Zbtb16* were obtained from SA Biosciences (Qiagen). Primer sequences for *Il2rb*: (f) 5′-caagtcgaacctgcgac (r) 5′-gatgcctgcctcacaag; *Id2*: (f) 5′- tgaacacggacatcagcatc (r) ccacagagtactttgctatcattcg. Primers were designed using Primer3. qPCR was performed on a Stratagene Mx3005p using Brilliant SYBR green master mix (Stratagene). Fold change values were calculated using the $2^{-\Delta\Delta Ct}$ method.

Acknowledgments

Egr-deficient mice were kindly provided by P. Charnay (INSERM, France). We thank E. Bartom for help with analysis of ChIP-Seq data, M. Wang for help with statistical analyses, the University of Chicago Animal Resource

Center, Core Flow Cytometry Facility, DNA Sequencing Facility; the NIAID tetramer facility for CD1d tetramers. This study greatly benefitted from the data assembled by the Immgen Consortium. The work was supported by NIH grants AI038339 and AI053725 and by the Digestive Disease Research Core Center P30 DK42086. M.P.S received support from an NRSA T32AI0709030 postdoctoral fellowship. R.M. is supported by an Irvington institute fellowship from the Cancer Research Institute. A.B. is a Howard Hughes Medical Institute Investigator.

References

1. Godfrey DI, Stankovic S, Baxter AG. Raising the NKT cell family. Nat Immunol. 2010; 11:197–206. [PubMed: 20139988]
2. Bendelac A, Savage PB, Teyton L. The biology of NKT cells. Annu Rev Immunol. 2007; 25:297–336. [PubMed: 17150027]
3. Benlagha K, Wei DG, Veiga J, Teyton L, Bendelac A. Characterization of the early stages in thymic NKT cell development. Journal of Experimental Medicine. 2005; 202:485–492. [PubMed: 16087715]
4. Savage AK, et al. The transcription factor PLZF directs the effector program of the NKT cell lineage. Immunity. 2008; 29:391–403. [PubMed: 18703361]
5. Kovalovsky D, et al. The BTB-zinc finger transcriptional regulator PLZF controls the development of invariant natural killer T cell effector functions. Nat Immunol. 2008; 9:1055–1064. [PubMed: 18660811]
6. Thomas SY, et al. PLZF induces an intravascular surveillance program mediated by long-lived LFA-1-ICAM-1 interactions. J Exp Med. 2011; 208:1179–1188. [PubMed: 21624939]
7. Raberger J, et al. The transcriptional regulator PLZF induces the development of CD44 high memory phenotype T cells. Proc Natl Acad Sci U S A. 2008; 105:17919–17924. [PubMed: 19004789]
8. Savage AK, Constantinides MG, Bendelac A. Promyelocytic leukemia zinc finger turns on the effector T cell program without requirement for agonist TCR signaling. J Immunol. 2011; 186:5801–5806. [PubMed: 21478405]
9. Shao H, Kono DH, Chen LY, Rubin EM, Kaye J. Induction of the early growth response (Egr) family of transcription factors during thymic selection. J Exp Med. 1997; 185:731–744. [PubMed: 9034151]
10. Carter JH, Lefebvre JM, Wiest DL, Tourtellotte WG. Redundant role for early growth response transcriptional regulators in thymocyte differentiation and survival. J Immunol. 2007; 178:6796–6805. [PubMed: 17513727]
11. Lawson VJ, Weston K, Maurice D. Early growth response 2 regulates the survival of thymocytes during positive selection. Eur J Immunol. 2010; 40:232–241. [PubMed: 19877014]
12. Lazarevic V, et al. The gene encoding early growth response 2, a target of the transcription factor NFAT, is required for the development and maturation of natural killer T cells. Nat Immunol. 2009; 10:306–313. [PubMed: 19169262]
13. Hu T, Gimferrer I, Simmons A, Wiest D, Alberola-Ila J. The Ras/MAPK pathway is required for generation of iNKT cells. PLoS One. 2011; 6:e19890. [PubMed: 21572967]
14. Laslo P, et al. Multilineage transcriptional priming and determination of alternate hematopoietic cell fates. Cell. 2006; 126:755–766. [PubMed: 16923394]
15. Rengarajan J, et al. Sequential involvement of NFAT and Egr transcription factors in FasL regulation. Immunity. 2000; 12:293–300. [PubMed: 10755616]
16. Bendelac A, et al. CD1 recognition by mouse NK1+ T lymphocytes. Science. 1995; 268:863–865. [PubMed: 7538697]
17. Zhou D, et al. Lysosomal glycosphingolipid recognition by NKT cells. Science. 2004; 306:1786–1789. [PubMed: 15539565]
18. Griewank K, et al. Homotypic interactions mediated by Slamf1 and Slamf6 receptors control NKT cell lineage development. Immunity. 2007; 27:751–762. [PubMed: 18031695]
19. Swirnoff AH, Milbrandt J. DNA-binding specificity of NGFI-A and related zinc finger transcription factors. Mol Cell Biol. 1995; 15:2275–2287. [PubMed: 7891721]

20. Townsend MJ, et al. T-bet regulates the terminal maturation and homeostasis of NK and Valpha14i NKT cells. Immunity. 2004; 20:477–494. [PubMed: 15084276]
21. Castillo EF, Acero LF, Stonier SW, Zhou D, Schluns KS. Thymic and peripheral microenvironments differentially mediate development and maturation of iNKT cells by IL-15 transpresentation. Blood. 2010; 116:2494–2503. [PubMed: 20581314]
22. Matsuda JL, et al. Homeostasis of V alpha 14i NKT cells. Nat Immunol. 2002; 3:966–974. [PubMed: 12244311]
23. Ikawa T, Fujimoto S, Kawamoto H, Katsura Y, Yokota Y. Commitment to natural killer cells requires the helix-loop-helix inhibitor Id2. Proc Natl Acad Sci U S A. 2001; 98:5164–5169. [PubMed: 11296270]
24. Monticelli LA, et al. Transcriptional regulator Id2 controls survival of hepatic NKT cells. Proc Natl Acad Sci U S A. 2009; 106:19461–19466. [PubMed: 19884494]
25. Boos MD, Yokota Y, Eberl G, Kee BL. Mature natural killer cell and lymphoid tissue-inducing cell development requires Id2-mediated suppression of E protein activity. J Exp Med. 2007; 204:1119–1130. [PubMed: 17452521]
26. Doulatov S, et al. PLZF is a regulator of homeostatic and cytokine-induced myeloid development. Genes Dev. 2009; 23:2076–2087. [PubMed: 19723763]
27. Collins S, et al. Opposing regulation of T cell function by Egr-1/NAB2 and Egr-2/Egr-3. Eur J Immunol. 2008; 38:528–536. [PubMed: 18203138]
28. Gallo EM, et al. Calcineurin sets the bandwidth for discrimination of signals during thymocyte development. Nature. 2007; 450:731–735. [PubMed: 18046413]
29. Kreslavsky T, et al. TCR-inducible PLZF transcription factor required for innate phenotype of a subset of gammadelta T cells with restricted TCR diversity. Proc Natl Acad Sci U S A. 2009; 106:12453–12458. [PubMed: 19617548]
30. Moran AE, et al. T cell receptor signal strength in Treg and iNKT cell development demonstrated by a novel fluorescent reporter mouse. J Exp Med. 2011; 208:1279–1289. [PubMed: 21606508]
31. Veillette A, Dong Z, Latour S. Consequence of the SLAM-SAP signaling pathway in innate-like and conventional lymphocytes. Immunity. 2007; 27:698–710. [PubMed: 18031694]
32. Fedeli M, et al. Dicer-dependent microRNA pathway controls invariant NKT cell development. J Immunol. 2009; 183:2506–2512. [PubMed: 19625646]
33. Wu Q, et al. MiR-150 promotes gastric cancer proliferation by negatively regulating the pro-apoptotic gene EGR2. Biochem Biophys Res Commun. 2010; 392:340–345. [PubMed: 20067763]
34. Bendelac A, Bonneville M, Kearney JF. Autoreactivity by design: innate B and T lymphocytes. Nat Rev Immunol. 2001; 1:177–186. [PubMed: 11905826]
35. Hayday AC. Gammadelta T cells and the lymphoid stress-surveillance response. Immunity. 2009; 31:184–196. [PubMed: 19699170]
36. Lambolez F, Kronenberg M, Cheroutre H. Thymic differentiation of TCR alpha beta(+) CD8 alpha alpha(+) IELs. Immunol Rev. 2007; 215:178–188. [PubMed: 17291288]
37. Kronenberg M, Rudensky A. Regulation of immunity by self-reactive T cells. Nature. 2005; 435:598–604. [PubMed: 15931212]
38. Wu Y, et al. FOXP3 controls regulatory T cell function through cooperation with NFAT. Cell. 2006; 126:375–387. [PubMed: 16873067]
39. Ruan Q, et al. Development of Foxp3(+) regulatory t cells is driven by the c-Rel enhanceosome. Immunity. 2009; 31:932–940. [PubMed: 20064450]
40. Zheng Y, et al. Role of conserved non-coding DNA elements in the Foxp3 gene in regulatory T-cell fate. Nature. 2010; 463:808–812. [PubMed: 20072126]
41. Turchinovich G, Hayday AC. Skint-1 Identifies a Common Molecular Mechanism for the Development of Interferon-gamma-Secreting versus Interleukin-17-Secreting gammadelta T Cells. Immunity. 2011
42. Singer A, Adoro S, Park JH. Lineage fate and intense debate: myths, models and mechanisms of CD4- versus CD8-lineage choice. Nat Rev Immunol. 2008; 8:788–801. [PubMed: 18802443]
43. Sciammas R, et al. An incoherent regulatory network architecture that orchestrates B cell diversification in response to antigen signaling. Mol Syst Biol. 2011; 7:495. [PubMed: 21613984]

44. Heng TS, Painter MW. The Immunological Genome Project: networks of gene expression in immune cells. Nat Immunol. 2008; 9:1091–1094. [PubMed: 18800157]
45. Ovcharenko I, Nobrega MA, Loots GG, Stubbs L. ECR Browser: a tool for visualizing and accessing data from comparisons of multiple vertebrate genomes. Nucleic Acids Res. 2004; 32:W280–286. [PubMed: 15215395]
46. Taillebourg E, Buart S, Charnay P. Conditional, floxed allele of the Krox20 gene. Genesis. 2002; 32:112–113. [PubMed: 11857793]
47. Benlagha K, Weiss A, Beavis A, Teyton L, Bendelac A. In vivo identification of glycolipid antigen specific T cells using fluorescent CD1d tetramers. J Exp Med. 2000; 191:1895–1903. [PubMed: 10839805]
48. Valouev A, et al. Genome-wide analysis of transcription factor binding sites based on ChIP-Seq data. Nat Methods. 2008; 5:829–834. [PubMed: 19160518]
49. Heinz S, et al. Simple combinations of lineage-determining transcription factors prime cis-regulatory elements required for macrophage and B cell identities. Mol Cell. 2010; 38:576–589. [PubMed: 20513432]
50. Kent WJ, et al. The human genome browser at UCSC. Genome Res. 2002; 12:996–1006. [PubMed: 12045153]

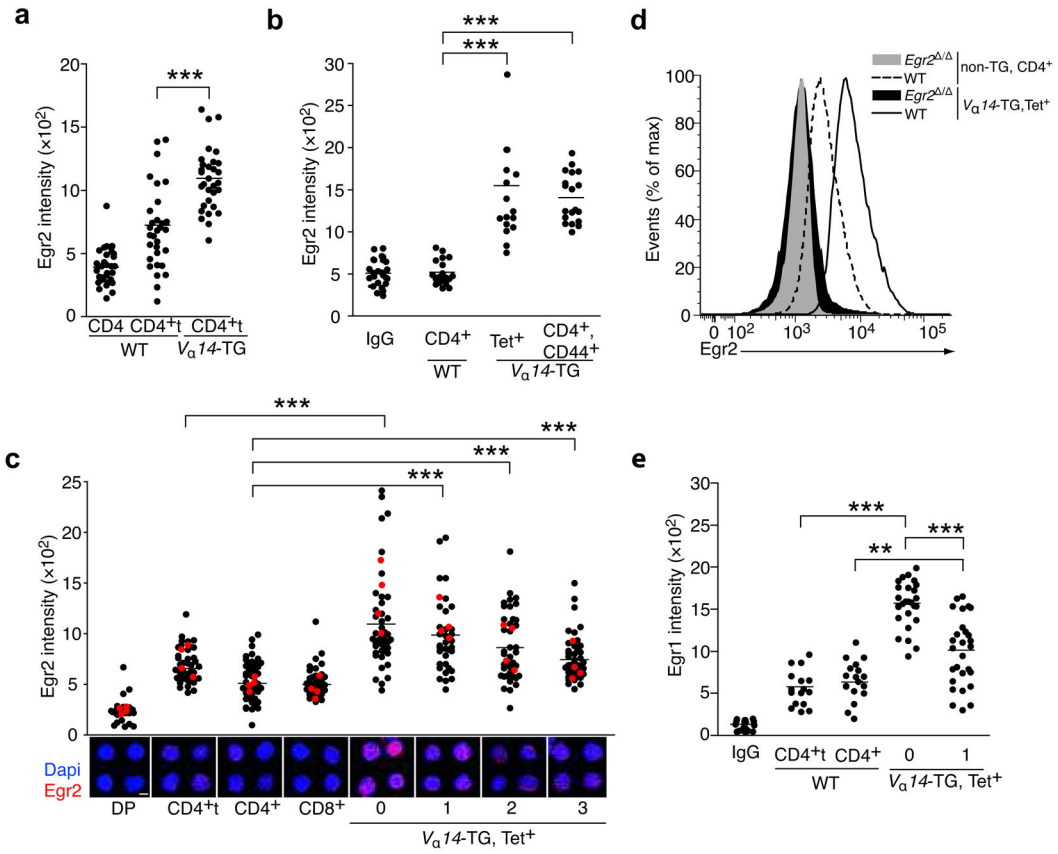

Figure 1. Elevated and prolonged Egr2 expression in NKT thymic precursors

(**a**) Fluorescence intensity for Egr2 measured by confocal microscopy in individual cells isolated from wild-type (WT) and $V_{\alpha}14$ transgenic ($V_{\alpha}14$-TG) mice into $CD4^+$ and $CD4^+$ transitional ($CD4^+$t) thymocyte subsets as indicated. (**b**) Fluorescence intensity for Egr2 measured by confocal microscopy in thymocytes sorted from wild-type mice as mature $CD24^{lo}CD4^+$ cells and from $V_{\alpha}14$-TG mice as $CD24^{lo}CD44^+NK1.1^-CD4^+$ (NKT stage 2) or as CD1d-αGalCer tet^+ (NKT stages 0 through 3) cells. Baseline staining of $V_{\alpha}14$-TG tet^+ thymocytes by IgG control is shown. (**c**) Fluorescence intensity for Egr2 measured by confocal microscopy in sorted $CD4^+CD8^+$ (DP), transitional $CD4^+$, mature $CD4^+$ and $CD8^+$ thymocytes from wild-type mice and in CD1d-αGalCer tet^+ NKT thymocytes sorted at stage 0 ($CD24^{hi}CD69^+$), stage 1 ($CD24^{lo}CD44^{lo}NK1.1^-$), stage 2 ($CD24^{lo}CD44^{hi}NK1.1^-$) and stage 3 ($CD24^{lo}CD44^{hi}NK1.1^+$) from $V_{\alpha}14$-TG mice. Red circles refer to the cells shown underneath the graph, scale bar = 5μm. (**d**) Intracellular flow cytometry staining of Egr2 in $CD4^+$ single positive thymocytes from wild-type (i.e. non-transgenic; non-TG) and $Egr2^{\Delta/\Delta}$ mice and in tet^+ thymocytes from $V_{\alpha}14$-TG and $Egr2^{\Delta/\Delta}$ $V_{\alpha}14$-TG mice. (**e**) Mean fluorescence intensity of Egr2 measured by confocal microscopy in individual $CD4^+$t and $CD4^+$ thymocytes sorted from wild-type mice and in stage 0 or stage 1 Tet^+ thymocytes sorted from $V_{\alpha}14$-TG mice. Baseline fluorescence level indicated by staining with control IgG. All results are representative of two (**b, e**) and three (**a, c, d**) independent experiments. Bars represent mean, $^{**}P<0.001$, $^{***}P<0.0001$ (two-tailed unpaired *t* test).

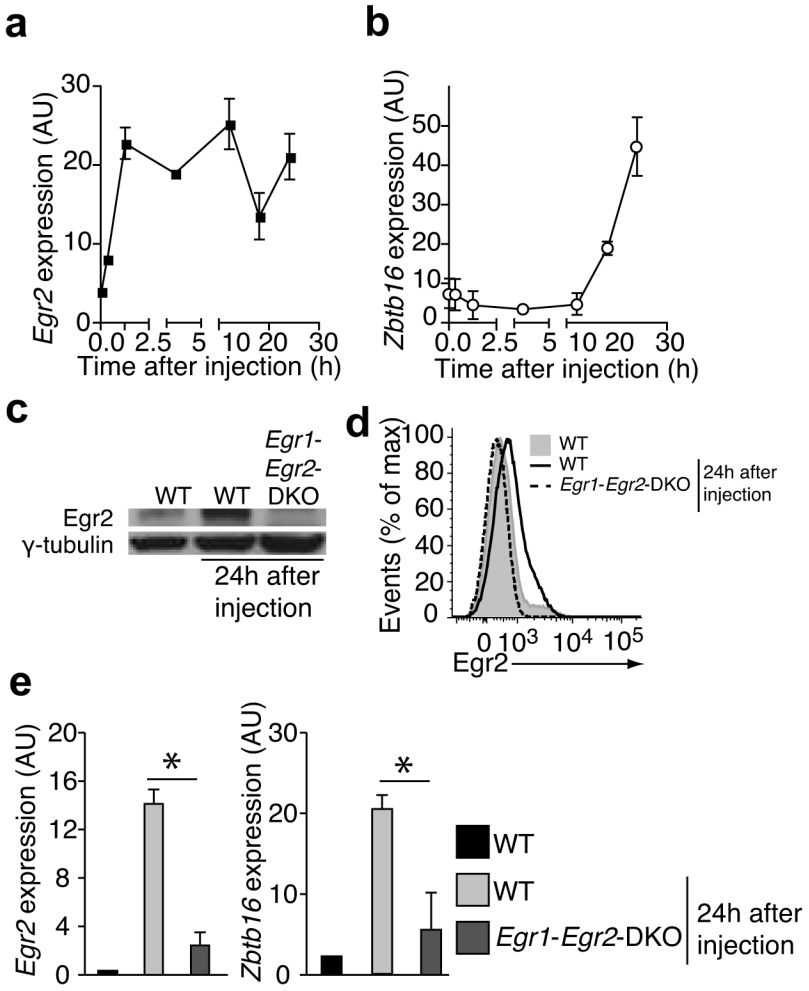

Figure 2. *Egr2* and *Zbtb16* induction in TCRβ-signaled thymocytes *in vivo*

qRT-PCR analysis of mRNA expression of *Egr2* (**a**) and *Zbtb16* encoding PLZF (**b**) in anti-CD69 MACs-enriched thymocytes collected at various time points post injection of 500 μg anti-TCRβ antibody in B6 mice. (**c**) Western blot analysis of Egr2 expression in whole thymocytes at 0 and 24 hours after anti-TCRβ injection in WT mice and in *Egr1-Egr2*-DKO mice. (**d**) Egr2 protein measured by flow cytometry of WT and *Egr1-Egr2*-DKO DP thymocytes before and 24 hours post injection of anti-TCRβ. (**e**) qRT-PCR analysis of thymocyte *Egr2* and *Zbtb16* mRNA after anti-TCRβ injection into WT or *Egr1-Egr2*-DKO mice. Data are representative of 3–5 independent experiments including 7 WT and 5 *Egr1-Egr2*-DKO mice. **P*<0.05.

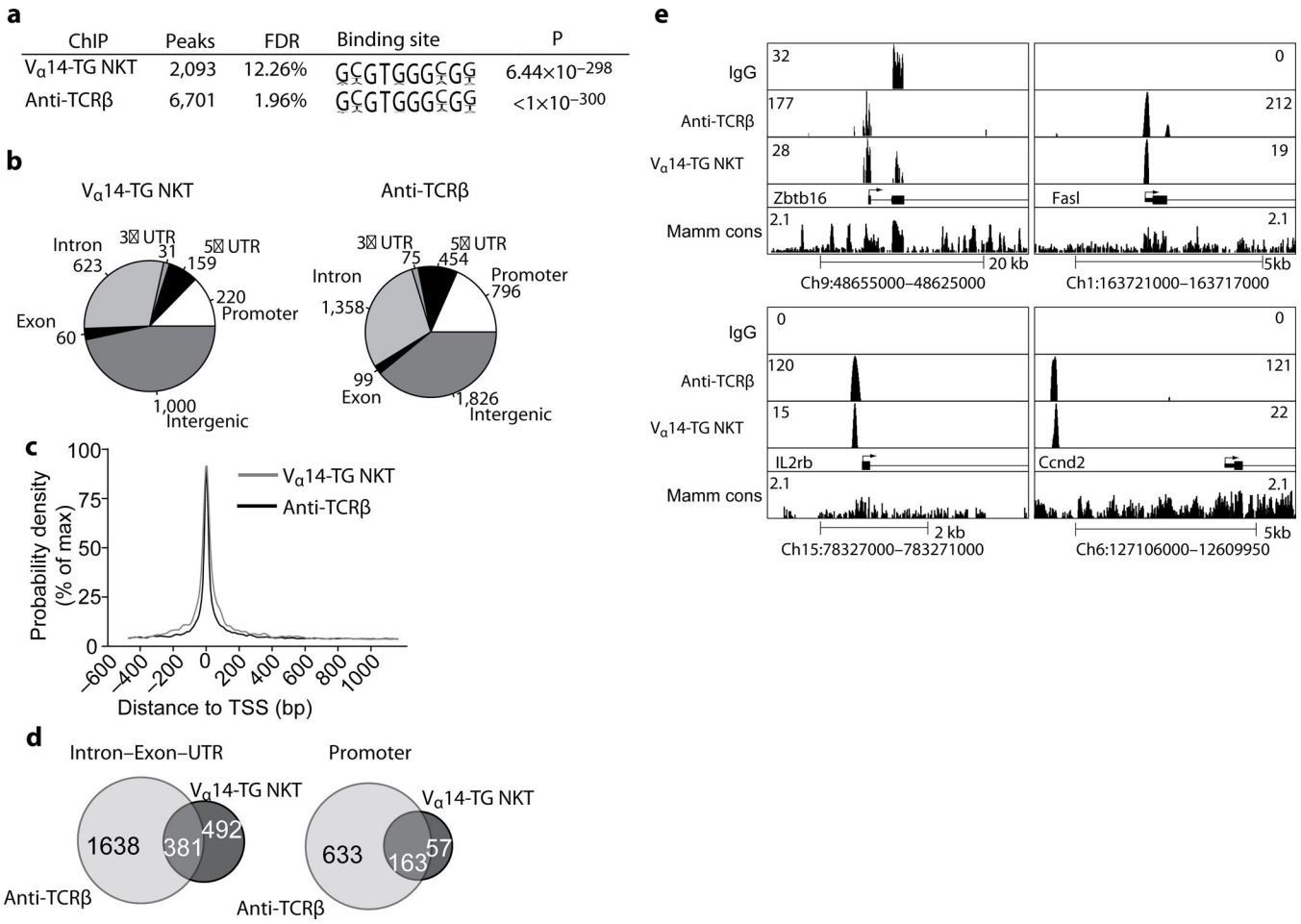

Figure 3. ChIP sequencing of Egr2 binding sites

(**a**) Egr2 ChIP-sequencing of CD1d-αGalCer$^+$ NKT thymocytes purified from pools of *Vα14*-TG mice, and of whole thymocytes from anti-TCRβ injected WT mice. Summary of all ChIP-seq datasets and *de novo* Egr2 binding motif; FDR, false discovery rate. (**b**) Peak distribution of Egr2 binding sites and (**c**) relative enrichment frequency near transcription start sites (TSS) in NKT thymocytes and anti-TCRβ injected WT thymocytes. (**d**) Overlap between promoter bound genes and between intron/exon/UTR regions in the two datasets. Overlap between intergenic sequences (38%) is not shown. (**e**) Peaks associated with *Zbtb16*, *Fasl*, *Il2rb*, *Ccnd2* in the two Egr2 ChIP Seq data sets and the IgG control.

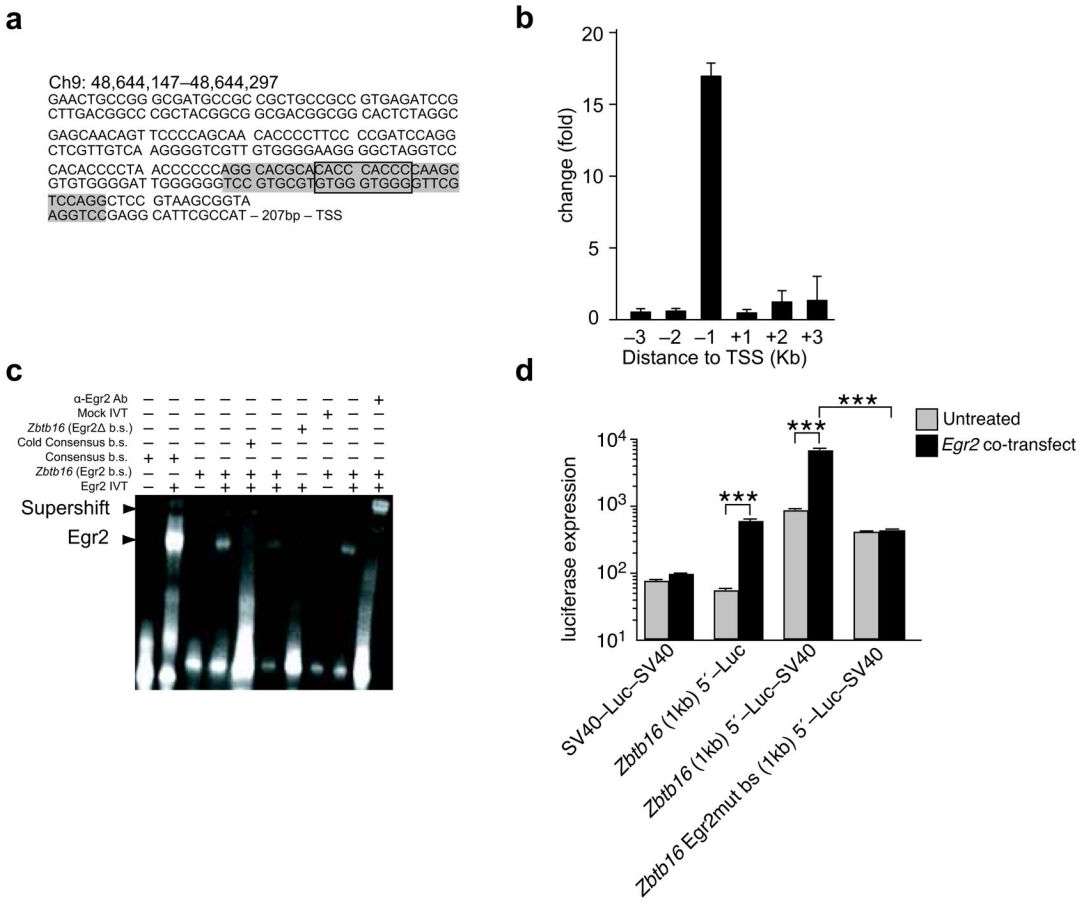

Figure 4. Egr2 binds and transactivates the *Zbtb16* promoter

(**a**) Identification of the putative Egr2-bound sequence in the 1kb region upstream of the *Zbtb16* TSS (black box). Shaded sequence is the oligonucleotide used in the gel shift showed in (c). (**b**) ChIP-qPCR validation of Egr2 binding to the 1kb region upstream of the *Zbtb16* transcription start site in chromatin isolated from $V_{\alpha}14$-TG NKT cells. Data are representative of 2 experiments, average fold change in site occupancy compared to input control. (**c**) Gel shift analysis showing binding of *in vitro* translated Egr2 to the *Zbtb16* promoter oligonucleotide carrying the Egr2-binding site (Egr2 bs), abrogation of binding to the oligonucleotide with mutated binding site (Egr2Δ bs) and supershift with anti-Egr2 antibody. Binding to an oligonucleotide with a consensus Egr2 bs and competition with cold consensus are shown as controls. Data are representative of 5 experiments. (**d**) Luciferase reporter assay of KG1a cells transfected with different *Zbtb16*-promoter driven luciferase expression plasmids with or without co-transfection of a pCMV-*Egr2* expression plasmid as indicated in the figure. Graph indicates mean and SEM, significance determined by unpaired student's t test. Data representative of 2 to 3 experiments with 4 replicates per condition. ***P<0.0001.

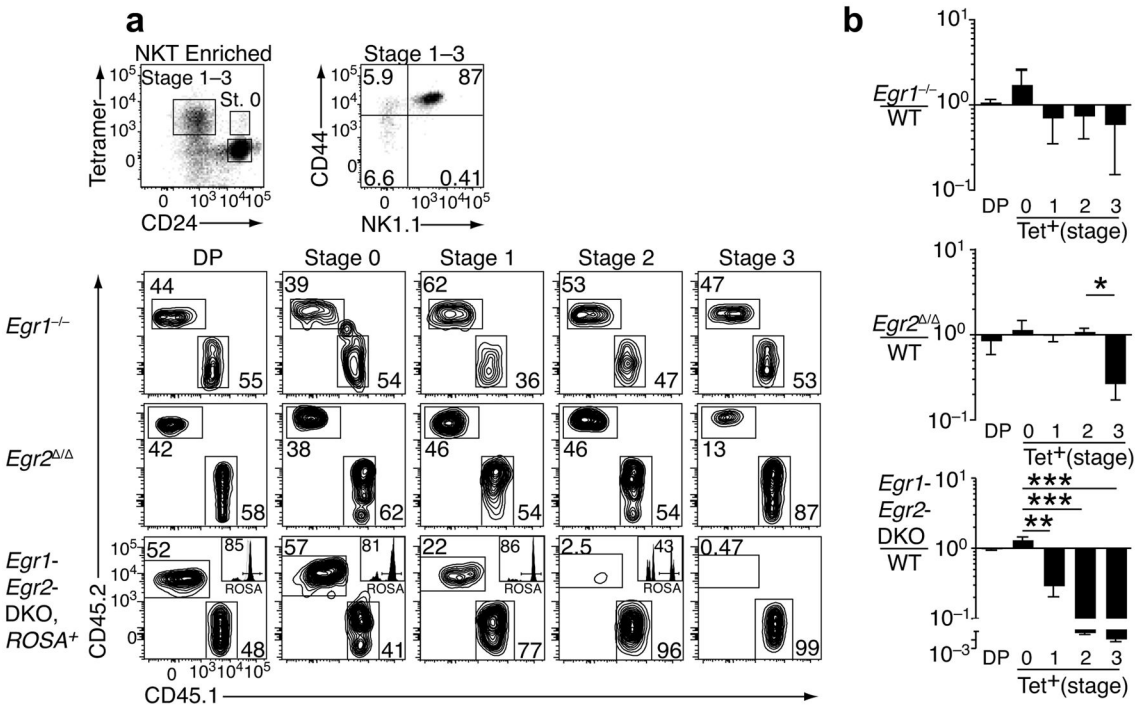

Figure 5. Egr2 controls early and late NKT developmental checkpoints

(**a**) Radiation bone marrow chimeras reconstituted with 1:1 mixture of WT (CD45.1) and either *Egr1*$^{-/-}$ (n=4), *Egr2*$^{fl/fl}$*lck-Cre*$^{+}$ (*Egr2*$^{\Delta/\Delta}$) (n=6) or *Egr1- Egr2*$^{\Delta/\Delta}$ ROSA26^{+} (n=6) (CD45.2) bone marrows, as indicated, were enriched for thymic CD1d-αGalCer^{+} NKT cells by tetramer-based MACS and analyzed for developmental progression along stages 0, 1, 2 and 3 as indicated. Inlays indicate % ROSA26 positive cells in the gated CD45.2 compartment, as a measure of creexcision efficiency. (**b**) Cumulative analysis of NKT thymic developmental stages in competitive bone marrow chimeras. Bar graphs show means and SD of mutant/WT ratios. P values determined by two-tailed paired t test. **P*<0.05, ***P*<0.001, ****P*<0.0001.

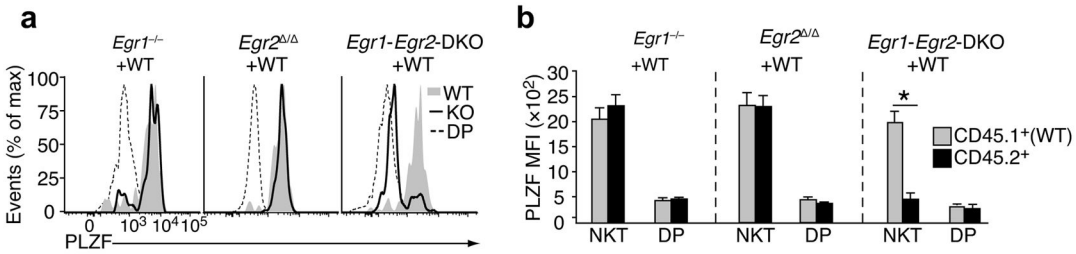

Figure 6. Egr2 is required for PLZF activation in NKT development

Representative histograms of PLZF expression in stage 1 NKT thymocytes of mutant and WT origin in competitive chimeras from figure 5. (**b**) Quantitative analysis of PLZF expression (mean fluorescence intensity) in stage 1 NKT cells from chimeric mice. Data representative of n=3 chimeras per condition. P values determined by two-tailed unpaired t test, **P*<0.05.

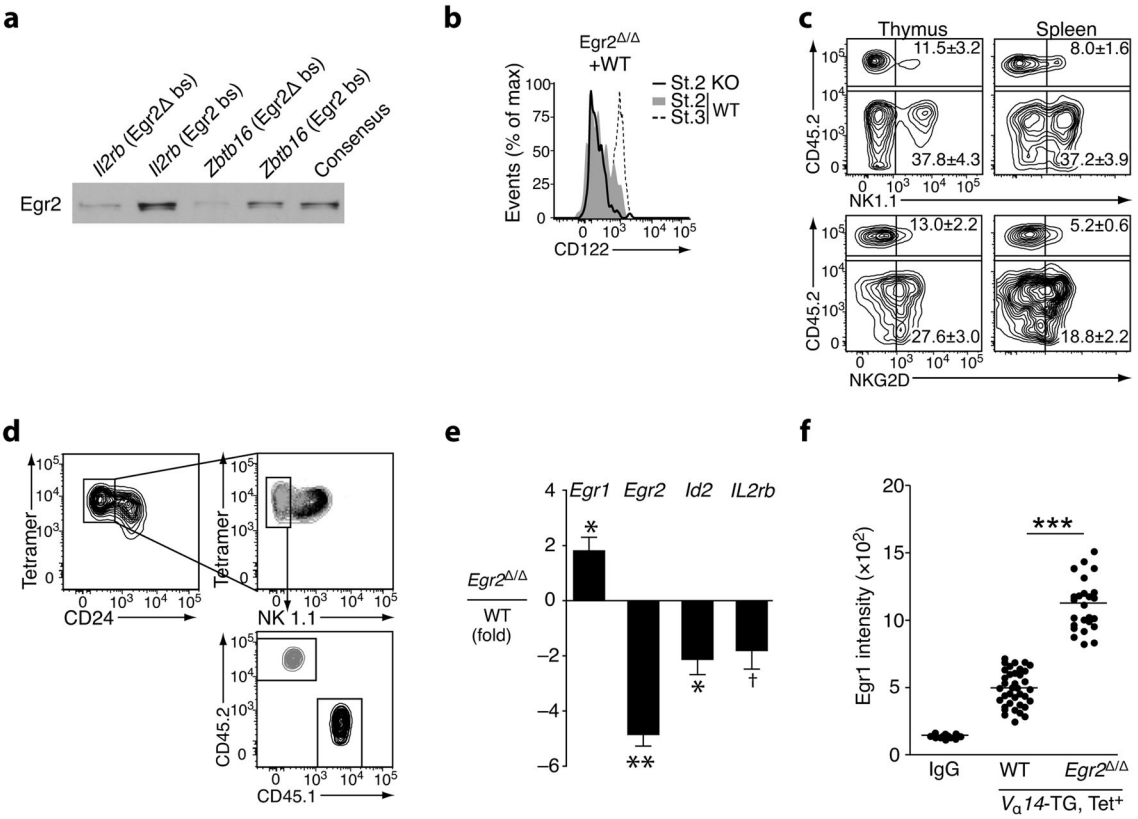

Figure 7. Egr2 is required for the stage 2 to stage 3 developmental transition

(**a**) Anti-Egr2 western blot after streptavidin bead precipitation of in vitro translated Egr2 protein pre-incubated with biotinylated double stranded oligonucleotides containing (Egr2 bs) or lacking (Egr2Δ bs) the putative Egr2 binding sequence. Oligonucleotide sequences are from the *Il2rb* and *Zbtb16* promoters as indicated, or represent a consensus Egr2 binding site. Representative of two independent experiments. (**b**) Expression of CD122 in stage 2-arrested Egr2-deficient CD1d-αGalCer^{+} thymocytes compared with stage 2 and stage 3 from WT CD1d-αGalCer^{+} thymocytes within the same competitive chimeras. Representative of 5 individual mixed chimeras. (**c**) Expression of NK1.1 and NKG2D by CD24^{lo}CD1d-αGalCer^{+} cells in Egr2-deficient $V_{\alpha}14$-TG thymocytes (KO, CD45.2^{+}) compared with Egr2-sufficient $V_{\alpha}14$-TG NKT thymocytes (WT, CD45.2^{-}) within the same competitive chimera. Data representative of 5 individual mixed chimeras and two independent experiments. (**d**) Sort strategy for stage (1 + 2) $V_{\alpha}14$-TG NKT cells from the WT and Egr2-deficient compartments of mixed chimeras analyzed by qRT-PCR in (e). CD1d-αGalCer tetramer MACS-enriched NKT cells were sorted as CD24^{lo} NK1.1^{-} cells of Egr2 sufficient (CD45.1^{+}, black contours) or Egr2-deficient (CD45.2^{+}, grey contours) origins. (**e**) Expression levels of indicated genes plotted as fold change in Egr2-deficient over wild type cells. Data summarize three independent qRT-PCR experiments with pools of 3–5 chimeras. **(f)** Confocal microscopic analysis of Egr1 fluorescence intensity in individual $V_{\alpha}14$-TG Tet^{+} thymocytes of Egr2-sufficient (WT) or Egr2-deficient origin in chimeras. Baseline

fluorescence indicated by staining with control IgG. P-values determined by two-tailed unpaired *t* test. **P*<0.05, ***P*<0.001, ****P*<0.0001, †*P*=0.08.

Table I

Identification of Egr2 target genes

Genes upregulated (>1.8 fold, $p<0.05$) at different stages of NKT development over CD4 SP thymocytes, were compiled from the Immgen consortium microarray datasets [44] and further selected based on binding by Egr2 in the ChIP-Seq datasets obtained from $V_{\alpha}14$-TG NKT thymocytes and from anti-TCRβ injected WT thymocytes. The final gene list was limited to those exhibiting a conserved Egr binding motif in human within 200 bp of the ChIP-Seq called binding site using the ECR browser, online informatics tool [45].

	NKT Stage		
	1	**2**	**3**
Upregulated genes in NKT/CD4	643	983	614
Bound by Egr2 in Vα14-TG NKT	33	43	41
Bound by Egr2 in anti-TCRβ	13	17	16
Conserved bs in human	5	7	7
	Zbtb16	*Zbtb16*	*Zbtb16*
	Il2rβ	*Il2rβ*	*Il2rβ*
		Ccnd2	
		Fasl	*Fasl*
		Fam46a	*Fam46a*
	Slc9a9	*Slc9a9*	*Slc9a9*
	Ptprv	*Ptprv*	*Ptprv*
	Hivep3		*Tbkbp1*